Thermal Design of a Mars Helicopter Technology Demonstration Concept

Tyler M. Schmidt[1], Stefano Cappucci[2], Jennifer R. Miller[3], Mark F. Wagner[4], Pradeep Bhandari[5], and Michael T. Pauken[6]
Jet Propulsion Laboratory, California Institute of Technology, Pasadena, CA 91109

The Mars Helicopter is a technology demonstration concept for a Mars surface mission. The primary mission objective is to achieve several 90-second flights and capture visible light images via forward and nadir mounted cameras. These flights could possibly provide reconnaissance data for sampling site selection for other Mars surface missions. The helicopter could be powered by a solar array, which stores energy in secondary batteries for flight operations, imaging, communications, and survival heating. The helicopter thermal design is driven by minimizing survival heater energy while maintaining compliance with allowable flight temperatures in a variable thermal environment. This is accomplished by absorbing as much solar energy on the fuselage exterior as possible in the daytime while minimizing heat loss at night. The batteries and electronics are located inside the fuselage and are conductively isolated from supporting structure. A CO_2 gas gap between the electronics and the fuselage skin provides additional thermal isolation from temperature extremes and convection heat losses experienced by the fuselage. On non-flight sols, the thermal design meets all temperature requirements and worst case cold survival heater energy requirements. On flight sols, the thermal design meets temperature and survival energy requirements as well as warmup energy requirements for the propulsion motors and servos. Sensitivity cases were analyzed for parametric variation in the convection coefficient, the fuselage optical properties, and time of day for flight. Thermal balance and limited protoflight testing of an engineering development model was also conducted to correlate the analytical thermal model and verify the thermal design. Using test data, several improvements were made to the thermal design to further reduce survival energy.

Nomenclature

α	=	solar absorptivity
ε	=	infrared emissivity
h	=	convection coefficient (W/m^2K)
k	=	thermal conductivity (W/mK)
L_S	=	solar longitude (°)
τ	=	Mars optical depth

I. Introduction

THE Mars Helicopter is a class D technology demonstration concept being developed in a collaboration between the NASA Jet Propulsion Laboratory (Caltech/JPL) and AeroVironment, Inc. (AV). AV is delivering the propulsion hardware (rotor blades, servos, motors), while JPL is designing and integrating the other subsystems. The helicopter concept would arrive at Mars as a deployable payload from a rover or lander type surface mission. Once deployed and operating nominally, the helicopter would fly several times for up to 90 seconds per flight. Two cameras

[1] Thermal Engineer, Spacecraft Thermal Engineering, 4800 Oak Grove Drive, Pasadena, CA 91109, M/S 125-123.
[2] Thermal Engineer, Thermal Fluid Systems and Mission Operations, M/S 125-123.
[3] Thermal Engineer, Spacecraft Thermal Engineering, M/S 125-123.
[4] Thermal Engineer, Thermal Fluid Systems and Mission Operations, M/S 125-123.
[5] Principal Thermal Engineer, Propulsion, Thermal, and Materials Systems, M/S 125-123.
[6] Senior Thermal Engineer, Thermal Fluid Systems and Mission Operations, M/S 125-123.

could capture visible light images from the forward and nadir sides of the fuselage. Current and planned Mars surface missions can use these reconnaissance images to aid terrain navigation or selection of sampling sites. Additionally, the helicopter can traverse and study terrain that would be inaccessible to rover or lander missions.

Since Mars's atmosphere is less than 1% as dense as Earth's (Ref. 1), achieving sufficient lift for flight drives the helicopter design (Figure 1). Thus, the helicopter mass is limited to approximately 2 kg for the current mission design capability. The mass constraint also limits the total available energy on board to approximately 28 Watt-hours (Wh) per sol in the best case. Energy is provided by six secondary batteries, which are recharged by a 0.14 m^2 solar array located above the upper set of blades. With only 28 Wh of total energy available per charge and facing a dynamic thermal environment on Mars, the thermal design must satisfy a demanding balance between energy conservation and positive margin for all allowable flight temperature (AFT) requirements.

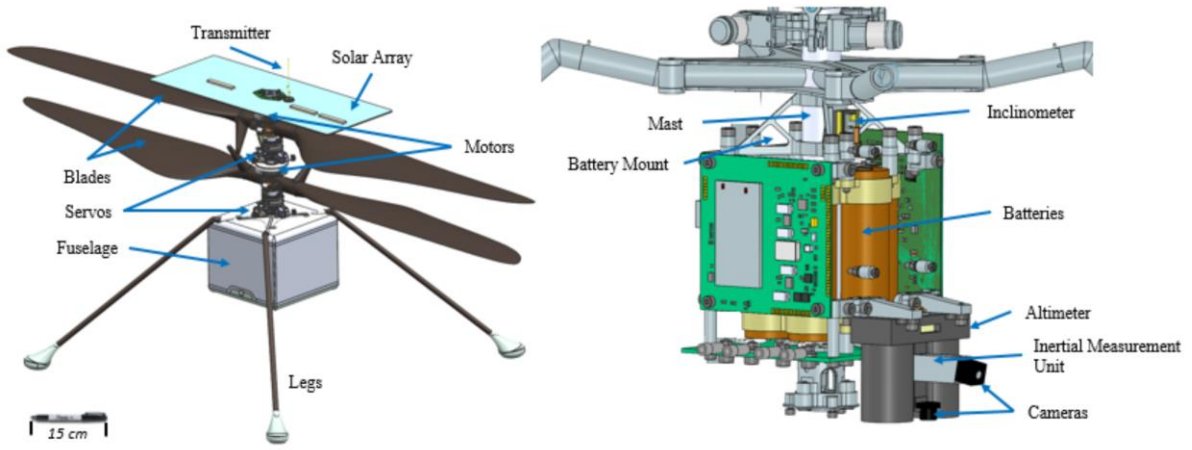

Figure 1. Model images of the helicopter concept. The left image shows the exterior components with a marker shown for scale. The right image shows the interior components, including the printed wiring boards, cameras, sensors, and batteries (one of the boards is hidden so the batteries are visible).

II. Mission Design and Thermal Inputs

The primary mission objective is to have several 90-second flights. The helicopter would arrive at Mars as a deployable vehicle for a Mars surface mission, such as a rover or lander. The design of the deployment mechanism would depend on the mechanical architecture of the rover or lander mission and will not be discussed in this paper. After deployment, the helicopter would begin functional checkout of the power and telecom subsystems. On non-flight sols, the helicopter would stay in a low power mode to conserve energy while the secondary batteries charge for a flight. Just before a flight, the batteries, sensors, and propulsion components would be warmed from non-operational to operational AFTs. Then, the propulsion components would be powered on to spin at 2800 revolutions per minute (RPM) to enable flight. During the flights, two on-board cameras would capture visible light images and transmit them back to Earth after landing. Since the one-way transmission time between Earth and Mars is between 3 and 22 minutes, all flights must be autonomous. The estimated time to recharge the batteries for another flight is two sols. A nominal mission duration would be roughly one Mars month.

A. Thermal Environment

Hypothetical landing sites in Mars's northern (18.5 °N) and southern hemispheres (14.5 °S) were originally considered. These sites were used since they bound a range of latitudes that contain several Mars surface missions, such as Mars Exploration Rovers Spirit and Opportunity (Ref. 2), Mars Science Laboratory (Ref. 3), and Mars InSight (Ref. 4). The transient temperature and solar flux profiles for both landing sites sites were developed from the Mars global circulation model (GCM) over the range of dates first considered for the nominal mission timeline, which was from solar longitude (L_S) 5° to 48°. This range was selected since L_S = 5° occurs just after the beginning of northern spring (vernal equinox), which results in a benign thermal environment compared to that of summer or winter. The lower and upper bounds for several categories of environment data are captured in Table 1. For the timeframe under consideration, the southern site contained both the driving hot and cold environments.

From L_S = 5° to 48°, Mars is approaching its aphelion (L_S = 71°). Therefore, as the mission timeline progresses, northern hemisphere solar flux is received at a progressively decreasing incident angle but at lower magnitude. This combination results in a somewhat constant solar flux and temperature profile over the mission. Conversely, in the southern hemisphere, solar flux is received at a progressively increasing incident angle and lower magnitude. This combination results in a steady decrease in solar flux and temperature over the mission. In this way, the northern landing site's environment is actually a subset of the southern site environment. If the design can meet thermal requirements in the southern site, there will be additional margin at most other locations between the landing site latitudes under consideration.

Table 1. Environment data from the GCM for the two landing sites. Red denotes the overall driving hot environment; blue denotes the overall driving cold environment. This characterization was based on analysis from the helicopter detailed thermal model.

Northern Site (18.5 °N)						
Time	Limit	Sky T (°C)	Atm T (°C)	Ground T (°C)	Direct Flux (W/m^2)	Diffuse Flux (W/m^2)
L_S = 5°	MIN	-101	-71	-72	0	0
	MAX	-69	-25	-6	326	118
L_S = 48°	MIN	-104	-70	-72	0	0
	MAX	-73	-26	-9	313	104
Southern Site (14.5 °S)						
Time	Limit	Sky T (°C)	Atm T (°C)	Ground T (°C)	Direct Flux (W/m^2)	Diffuse Flux (W/m^2)
L_S = 5°	MIN	-112	-83	-85	0	0
	MAX	-84	-19	-2	338	102
L_S = 48°	MIN	-122	-92	-93	0	0
	MAX	-100	-39	-24	250	85

Wind speed data were also generated from the GCM. For the two landing sites and L_S range under consideration, the wind speed was almost bound between 0 and 10 m/s. Most importantly, the wind speed was predicted to drop close to 0 m/s for a portion of the morning around 1000 hours local time. This period of low wind conditions provides a daily window of opportunity for the helicopter to fly. At the height above the surface roughly equivalent to the fuselage, the wind speed in m/s translates to roughly one-fifth the convection coefficient, h, in W/m^2K. The convection coefficient during low wind conditions is approximately 0.4 W/m^2K due to natural convection.

$$\begin{cases} \boldsymbol{h = 0.4} & (\boldsymbol{wind < 2\frac{m}{s}}) \\ \boldsymbol{h = \frac{wind}{5}} & (\boldsymbol{2\frac{m}{s} < wind \leq 15\frac{m}{s}}) \end{cases} \quad (1)$$

Based on this system of equations and the GCM data, the no wind case (h = 0.4 W/m^2K) was typically used for hot cases, and a 10 m/s wind (h = 2 W/m^2K) was typically used for cold cases. These convection coefficients were applied over an entire diurnal period rather than using a transient profile. By using this approach, the analysis would be more bounding.

The southern and northern landing sites used thermal inertias of 228 and 336 $J/m^2/K/s^{0.5}$ respectively. The albedos were 0.23 and 0.17 respectively. An optical depth, τ, of 0.7 was used for both sites. An optical depth of 0.2 was also considered to generate GCM environment data, but tau of 0.7 was more driving on the thermal design in both the hot and cold cases. For the hot case, the helicopter receives more diffuse solar energy, which can be absorbed on all six sides of the fuselage. In the cold case, the helicopter simply receives less total (direct plus diffuse) solar energy.

B. Maximum Energy Available

Since the solar energy received (and extracted from the array) in the northern and southern hemispheres evolves over the mission, the maximum energy available from the batteries is variable. Figure 2 illustrates that the northern landing site has a larger and mostly constant energy allocation for most of the mission compared to that in the southern landing site. Since the southern hemisphere is approaching winter, the survival energy needed to control temperatures to AFTs will increase. As a result, the end of mission southern site environment represents the worst case for survival energy use.

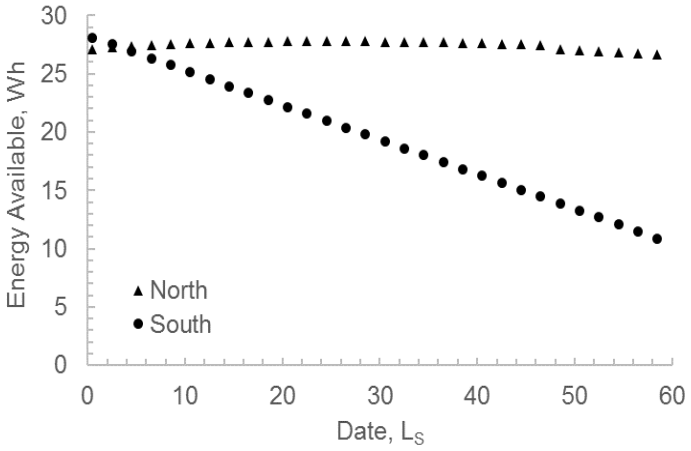

Figure 2. Maximum energy available in the batteries as a function of mission time.

C. Mission Operations and Constraints

Before a flight can occur, several environmental and operational constraints must be met:

Environment

- Sufficient lighting for cameras
- Wind speed must low enough for stable flight

Operations

- All sensors, including the inclinometer, cameras, and altimeter, must be warmed to lower limit operational AFT (-40 °C)
- Batteries must be warmed to lower limit operational AFT (+5 °C)
- There must be enough energy stored in batteries for warmup and flight so as to not drop below 28% state of charge post-flight

III. Thermal Design Architecture

The battery AFT limits are the primary drivers of the thermal design. At night, the batteries must be temperature controlled at the lower limit AFT by heaters. The electronic components on the printed wiring boards dissipate less than 10 Wh each non-flight sol, so the battery heater must provide supplemental energy to meet AFT requirements. During the day, the battery upper limit AFT bounds the solar energy that can be absorbed by the fuselage before the batteries overheat. Thus, a trade forms between absorbing solar energy as sensible heat while preventing overheating of the batteries. The majority of components outside the fuselage have much wider AFT limits and minimally affect the design and survival energy. As such, these components can be thermally isolated from the electronics inside the fuselage to prevent heat leaks.

Table 2. Temperature Requirements Table. All temperatures are °C.

	Operational		Non-Operational	
	Min	Max	Min	Max
Propulsion Subsystem				
Motors	-11	43	-77	44
Servos	-37	-1	-77	14
Sensors				
Altimeter	-25	50	-110	50
Cameras	-25	50	-110	50
Inertial Measurement Unit	-25	50	-110	50
Inclinometer	-25	50	-110	50
Electronics Core Module				
Battery	5	40	-15	40
Printed Wiring Boards	-40	50	-40	50
Exterior Components				
Fuselage	-23	23	-79	46
Blades	-40	10	-99	21
Solar Array	-105	50	-105	50
Mast	-49	40	-80	50

Some of the thermal requirements changed regularly during the design process. As the battery AFT limits were crucial to the thermal design, the lower limit changed periodically. For the current design, the non-operational lower limit AFT during the night is -15 °C while the operational lower limit AFT during a flight is +5 °C (Table 2). The battery upper limit AFT is firmly established at +40 °C. To help the reader follow the evolution of the design, the model predictions and testing sections of the paper are written in chronological order.

A. Batteries

Six off-the-shelf rechargeable batteries are the only electrical energy source for the helicopter. The non-operational AFT range is -15 to +40 °C, which drives the thermal design in both the cold and hot cases. The operational AFT range, which applies to charging and flight activities, is +5 to +40 °C. At night, the batteries must be temperature controlled at the lower AFT limit by kapton film heaters. The batteries are conductively coupled to each other with a pair of aluminum harnesses to help isothermalize the cells for similar performance. The harnesses are then thermally isolated from supporting structure by Ultem™ (polyetherimide, $k \approx 0.14$ W/mK) spacers and a titanium mount that interfaces with the mast. The thermal isolation scheme is described in more detail later on.

B. Fuselage

The helicopter fuselage is a 0.5 mil Kapton film material that surrounds the electronics and batteries. The exterior optical properties of the film were chosen through a trade study between margin against the battery upper limit AFT and minimizing survival energy. The outer surface of the fuselage is a dark film with nominal properties of $\alpha = 0.68$ and $\varepsilon = 0.06$ ($\alpha/\varepsilon \approx 11$). The high α/ε ratio maximizes solar energy absorption in the daytime while still meeting AFT requirements. The low emissivity limits heat loss in the nighttime when the battery survival heater is needed. The inside of the fuselage has a nominal $\varepsilon = 0.035$. This helps to further isolate and decouple the internal electronics and batteries, which have the most constraining AFT limits, from the fuselage, which is subject to more extreme diurnal

temperature changes. Additionally, this thermally decouples the electronics boards from local cold and hot spots on the fuselage, which is non-isothermal due to low thermal conductivity ($k \approx 0.1$ W/mK) of the Kapton film.

Mars is subject to occasional dust storms, which can affect optical properties of exterior components. Mars dust has a size on the order of 1 to 2 µm, which tends to bias the solar absorptivity (wavelengths ~ 0.5 µm) of a surface towards that of dust (0.7) while leaving the IR emissivity (wavelengths ~ 5 to 40 µm) relatively unchanged (Ref. 5). Since the fuselage has $\alpha \approx 0.68$, the dust should have minimal impact on the fuselage's absorptivity. Additionally, it is assumed any dust that accumulates on the fuselage will be removed each time the helicopter flies.

C. Thermal Isolation

Since the battery heaters are the only viable heat source for maintaining the batteries above their minimum AFT limit at night, the batteries must be well insulated to conserve energy. Therefore, the batteries are conductively isolated from the surrounding helicopter structure. This is achieved through the use of low thermal conductivity materials, such as titanium, Ultem™, and composites, as well as CO_2 gas gaps.

At bolted interfaces, Ultem™ spacers were used to reduce conductive heat leaks. The batteries are mounted to the mast with a titanium bracket. This bracket has a hollowed out geometry to reduce mass and thermal conductance.

The mast of the helicopter is the primary structural component to which the rest of the hardware is mounted. The mast is made of composite materials intended to meet structural (high strength) and thermal (low thermal conductivity) requirements. The mast is constructed of a composite material with $k \approx 4$ W/mK.

The helicopter legs will have a hollow tube geometry with a 1.5 mm wall thickness. The legs are also designed with a composite material, which will have low thermal conductivity. The leg design is still in development, but it is required to have a thermal resistance of at least 25 K/W per leg to minimize heat loss.

Lastly, there are CO_2 gas gaps, which are simply gaps between components that are open to the Mars atmosphere. The thermal conductivity of CO_2 at the temperatures expected in flight is on order of 0.01 W/mK, which provides conductive insulation of interior components from the fuselage. All of the gas gaps are large enough to take advantage of conductive isolation without being so large as to introduce convection, which starts to occur at gap widths of 6 or 7 cm (Ref. 6).

IV. Thermal Analysis and Trade Studies

Several trade studies were conducted to meet or improve margins against temperature and energy requirements. All thermal modeling was done in Thermal Desktop (model shown in Figure 3), with periodic checks being performed with simplified spreadsheet models and hand calculations. These trades generally occurred in series as the design matured.

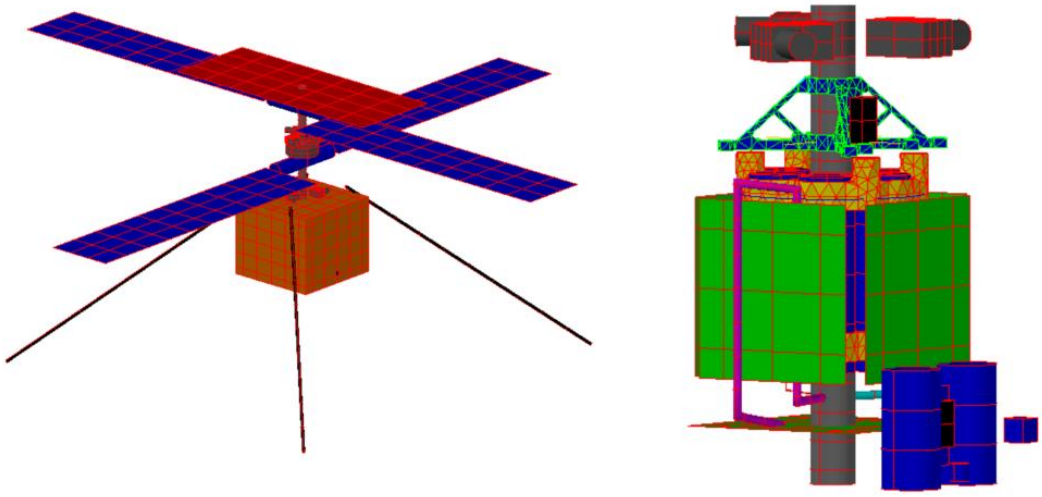

Figure 3. Images of the helicopter thermal model from the external (left) and internal (right) views.

A. Landing Site

If the design can meet all thermal requirements with positive margin in a variety of thermal environments, there will be more opportunities for the helicopter to participate in a suitable parent mission. The thermal model predictions (Table 3) for a nominal wind case (5 m/s) on a non-flight sol show that the design meets AFT requirements at both the northern and southern landing sites (only battery temperature predicts are shown since they are the most driving and usually have least margin). Over the entire mission, the design only has positive energy remaining at the northern site. At the end of mission time at the southern site, the helicopter requires 5.8 Wh beyond the energy available. Since the resources required to make the southern landing site viable were well beyond the design capability for even a nominal case, the southern site was eliminated from further design work.

Table 3. Temperature (°C) and energy predictions (Wh) for the northern and southern landing sites on a nominal (5 m/s wind speed), non-flight sol.

Site, Time	Max Batt T (°C)	T Margin (°C)	Survival Energy (Wh)	Available Energy (Wh)	Remaining Energy (Wh)
N, L_S = 5°	36	**+4**	10.2	27.4	**+17.2**
N, L_S = 48°	27	**+13**	9.9	27.5	**+17.6**
S, L_S = 5°	37	**+3**	13.5	27.0	**+13.5**
S, L_S = 48°	12	**+28**	19.8	14.0	**-5.8**

B. Aerogel Insulation

Another trade study investigated the use of aerogel between the electronics and fuselage as a means of providing greater thermal isolation than could be achieved by CO_2 gas gaps alone. The fuselage's external optical properties were also varied to measure any sensitivity to the energy differences. The aerogel implementation would be similar to that used on the Mars Exploration Rovers: the aerogel would be 25 mm thick, opacified with carbon, and covered with a gold or aluminum coated kapton film to limit heat loss by radiation (Ref. 7).

The energy (Wh) predictions for the aerogel vs CO_2 trade using a non-flight sol and nominal wind (5 m/s) case are shown in Table 4. All cases shown meet AFT requirements. The differences in temperatures among all test cases were within 1 °C. Overall, the aerogel was estimated to save approximately 2 Wh when other parameters were held constant. The primary effect of the aerogel design was a reduced duty cycle for the battery heater during the nighttime.

Although the aerogel could have saved around 2 Wh per sol, it was not pursued for several reasons. First, the added mass (50 g) of the aerogel, reflective surface film, and supporting hardware was unfavorable even when considering the possible energy savings. Second, the aerogel thermal properties are subject to workmanship and manufacturing. If defects form in the aerogel, the effective thermal conductivity could become higher than that of CO_2. Third, aerogel must be handled cautiously during implementation lest it be crushed and create a thermal short, which goes back to the second problem. Aerogel remains an opportunity for energy savings, but it is not part of the current thermal design.

Table 4. Survival energy (Wh) predictions for the northern landing site on a nominal wind (5 m/s) and non-flight sol as a function of aerogel presence and fuselage external optical properties. All cases shown satisfied AFT requirements with positive margin.

Solar Longitude	α/ε Values	α/ε Ratio	No Aerogel, Energy (Wh)	25 mm Aerogel, Energy (Wh)	Energy Savings (Wh)
L_S = 5°	0.60/0.03	20	15.8	13.8	**+2.0**
	0.30/0.03	10	18.6	16.6	**+2.0**
	0.60/0.10	6	17.3	15.3	**+2.0**
	0.30/0.10	3	20.1	18.2	**+1.9**
L_S = 48°	0.45/0.03	15	20.4	18.6	**+1.8**
	0.30/0.03	10	22.0	20.1	**+1.9**
	0.45/0.10	4.5	22.6	20.2	**+2.4**
	0.30/0.10	3	24.3	22.1	**+2.2**

C. Wind Speed

The optical properties of the fuselage were tuned to produce a coating that could be made by the manufacturer. After several modeling iterations, a material with $\alpha = 0.68$, $\varepsilon = 0.06$ (α/ε was now approximately eleven) was adopted as the baseline fuselage material. These properties still satisfied all AFT requirements for flight and non-flight sols while minimizing survival energy.

The wind speed was varied as a robustness check on the thermal design. The bounding wind speed cases were 0 m/s and 10 m/s for the hot and cold case analyses respectively. The two hot cases included a 90-second flight at 1000 hours local time (time of flight was investigated in the next trade study).

The predictions for each of the cases are shown in Table 5. The thermal design meets AFT and energy requirements in each case with the exception of the worst case hot. In the no wind case, the battery temperature exceeds the upper limit AFT by 10 °C. However, in revisiting the no wind assumption, this was very conservative considering the GCM wind data. When considering the nominal hot case, there was 7 °C positive margin against the AFT requirement. Since the average wind speed over a sol for the mission lifetime is roughly 5 m/s, not meeting the driving hot case robustness check was acceptable given that the 3.5 m/s case demonstrated positive temperature and energy margin.

Table 5. Survival energy (Wh) and battery temperature (°C) predictions for a range of convection coefficients (W/m^2K). All analysis cases were for the northern landing site only.

Case	Wind Speed (m/s)	h (W/m^2K)	Max Battery T (°C)	Upper T Margin (°C)	Survival Energy (Wh)	Available Energy (Wh)	Energy Remaining (Wh)
Robustness Check Hot, L_s = 5°, flight	0	0.4	50	**-10**	10.9	27.4	**+16.5**
Nominal Hot, L_s = 5°, flight	3.5	0.7	33	**+7**	14.1	27.4	**+13.3**
Nominal Cold, L_s = 48°, non-flight	5	1	1	**+39**	19.6	27.5	**+7.9**
Robustness Check Cold, L_s = 48°, non-flight	10	2	-5	**+45**	25.0	27.5	**+2.5**

D. Flight Time of Day

The time of day for flight was analyzed as another trade. This impacts two aspects of the thermal design. First, it affects the amount of warmup energy needed for the batteries and sensors just before flight. If the flight occurs early in the day, more warmup energy is needed since the fuselage has not absorbed as much sensible heat from incoming solar energy. Second, it affects the latest time the helicopter can fly without overheating. Flying early in the day requires more warmup energy; flying later in the day risks overheating the batteries.

The thermal model was run for a low wind (3.5 m/s) flight sol case (same as "nominal hot" case parameters in Table 5). Several different times of day were considered for a 90-second flight. Figure 4 shows a plot of the maximum battery temperature as a function of these various flight times. The 2PM flight time results in an AFT violation by 4 °C, which makes flights around 2PM or later non-viable. Interestingly, the battery temperatures quickly converged in the late afternoon, which indicated that flying later in the day was not an opportunity to store energy approaching nighttime. Positive margin to the battery upper limit AFT was deemed more important than the potential warmup energy saved by flying later in the day. Therefore, the earliest flight time that does not produce a state of charge below 28% after the flight is best.

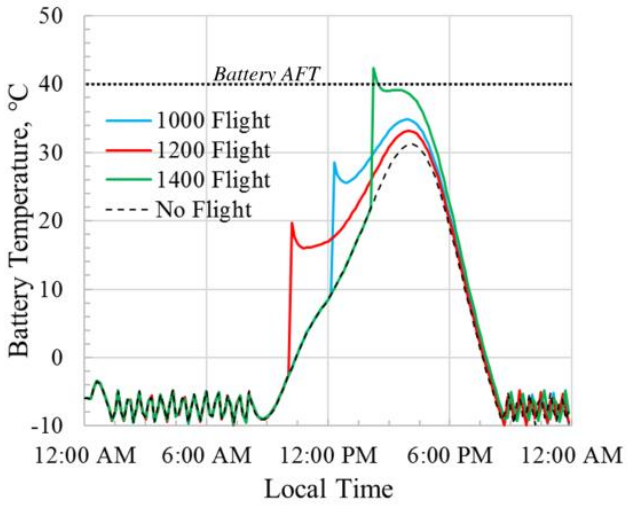

Figure 4. Parametric variation of the time of flight at the northern landing site.

V. Thermal Testing

A. Test Setup

An engineering model (EM) of the helicopter was used for thermal balance and limited protoflight testing in November 2017. The test featured three steady state thermal balance points (one in vacuum and two at Mars ambient pressure [6 to 10 torr (800 to 1333 Pa)]), several functional checkouts, and two short simulated flights. The vacuum case (pressure less than $1*10^{-5}$ torr [1.3 mPa]) was included to remove effects of convection and help model correlation. This test campaign also provided an opportunity to conduct protoflight testing of several components. The most critical thermal outcome was determining the survival energy needed for the cold steady state case.

The test was conducted in the ten foot horizontal chamber at JPL. The chamber was backfilled with N_2 to a pressure around 6 to 10 torr (800 to 1333 Pa) for the majority of testing. CO_2 was not used since it would freeze close to the lower qualification temperature limit (-125 °C) of the sensors. The helicopter was supported in the chamber by a welded aluminum stand (Figure 5). The stand was primarily designed to restrain the helicopter during a simulated flight. Since the helicopter was sensitive to heat leaks and accurate evaluation of the energy use was critical for this testing, the stand was also designed to thermally isolate the helicopter from the chamber

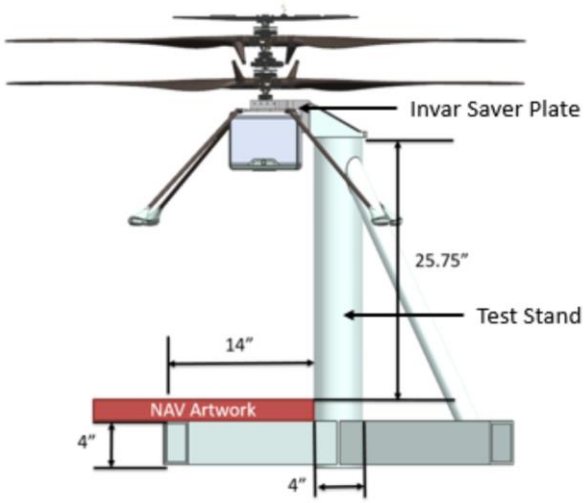

Figure 5. Test setup for helicopter. The test stand is a welded aluminum frame with an invar saver plate that interfaces with the helicopter mast. An artwork pattern below the helicopter provides a target for the nadir camera.

shroud. The stand interfaced with the helicopter's mast by an invar plate and several stainless steel fasteners that have Ultem™ washers (Figure 6).

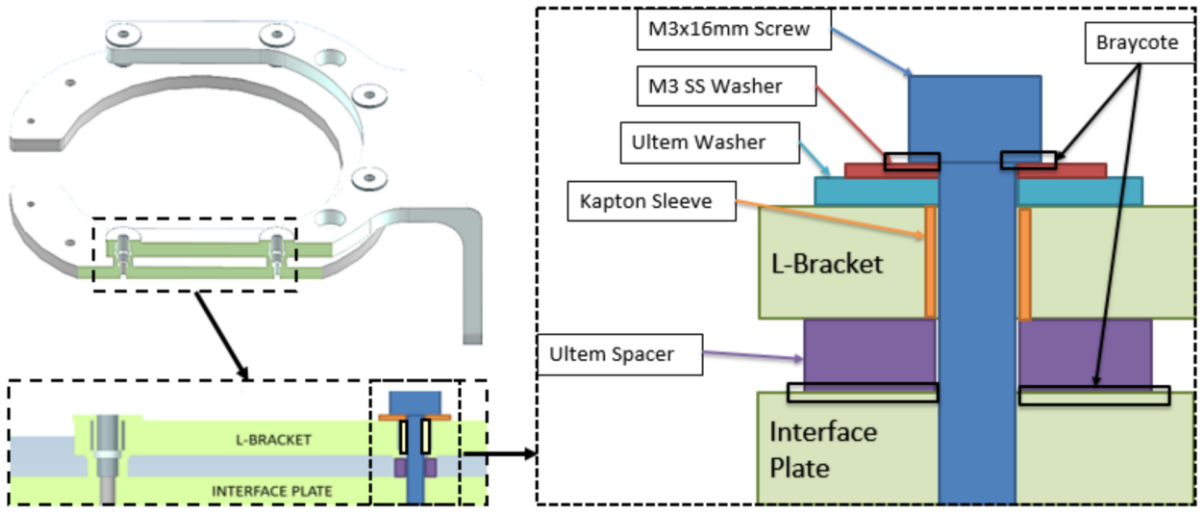

Figure 6. Thermal isolation scheme for the helicopter. The upper left image shows the L-bracket and interface plate where they would meet with the helicopter mast. The lower left image shows a cross section view of the interface with the middle saver plate layer included. The right image shows the thermal isolation scheme at the bolted interfaces.

B. Test Results

Overall, testing was successful for developing a correlated thermal model, collecting test data to characterize the as-tested thermal design, and demonstrating a short duration flight of an integrated EM unit. The pre-test thermal model predicts were correlated to test data within an average of 4 °C for all test thermocouples across all three test cases. Successful outcomes from testing include:

1. Determination of survival energy for a cold case in vacuum and at Mars ambient pressure
2. Demonstrated warm up of motor, servo, sensor packages, and batteries from non-operational to operational AFT limits in preparation for a simulated flight
3. Operated sensor packages at lower limit AFT
4. Started and operated FPGA at lower limit AFT
5. Conducted low speed flight test at 1500 RPM
6. Captured images at camera lower limit AFT
7. Successful operation of electronics and sensors after reaching lower limit PF
8. Performed operational tests of electronics at upper limit AFT

Using the correlated flight model and EM test specific parameters, the predicted survival energy for a cold case was almost 50 Wh, which far exceeded the available energy at any time in the mission. Although part of this energy growth was due to test-specific conditions that would not be present in flight, particularly extra ground support cables, testing did reveal that modifications were needed to reduce survival energy to an acceptable value. The following changes were specifically recommended by the thermal subsystem to reduce energy usage:

1. Reduce the battery heater set point from -10 °C to -15 °C since successful operation of the batteries was demonstrated at -25 °C; additionally, change the heater control to a flight software scheme so the deadband is reduced from 5 °C to 1 °C
2. Decrease the emissivity of the fuselage coating to reduce heat loss
3. Use a low emissivity coating on the batteries and the portion of the mast inside the fuselage
4. Add a low emissivity shield between the top of the batteries and top of the fuselage; this will prevent radiation heat loss through the opening at the top of the fuselage
5. Increase length of battery power cable by 50% to reduce the thermal conductance from batteries to printed wiring boards
6. An additional finding from testing was that the effective width of the CO_2 gas gaps was smaller than what was modeled. This was attributed to the presence of components of the boards (which was ignored in the

thermal model) and the challenge of creating accurate thermal model contactors between circular and rectilinear geometry. Larger gas gaps between the batteries and boards were also recommended as a way to reduce heater power.

The correlated thermal model was run using each of the above recommendations. The survival energy needed for a cold case was predicted at 21 Wh, which was within the energy available at the northern landing site. The design also meets all AFT requirements with positive margin for a nominal hot case with a flight at 1030 hours. At this point in the design, 1030 hours was the earliest predicted time the helicopter could fly without the batteries dropping below the minimum state of charge.

C. Future Thermal Testing

Additional testing will be performed to evaluate the effectiveness of the proposed recommendations and validate requirements not addressed in the first test campaign. The previous EM test focused on steady state thermal cases to assist with model correlation. Future testing will focus more on transients, mission operations scenarios, and longer duration flights. There will also be solar testing of the fuselage in order to verify the value of the solar absorptivity, which is important for storing sensible energy. The legs will also be included in future tests to verify they do not represent a major heat leak. Lastly, the battery design continues to mature with respect to temperature requirements and charging. Future tests will use a more flight-like battery charging sequence of operations. Additional protoflight and qualification testing will also be needed for hardware that was not qualified in this first thermal balance test.

VI. Future Work

The helicopter thermal design will continue to mature following changes made in response to EM thermal testing. Once the Mars Helicopter becomes a confirmed payload on an upcoming mission, thermal analysis will be needed for the cruise and surface deployment phases of the mission. The correlated thermal model can be used to generate predictions for these environments using interface temperatures and boundary conditions supplied by the parent mission. A deployment mechanism design can also be commissioned and tested. Lastly, the thermal analysis can be done for a certified landing site to verify that all requirements are still met. These analyses will be followed by thermal testing of the helicopter. This will provide a chance to validate additional requirements not addressed in the EM thermal balance testing and quantify the impact of modifications made after the first EM thermal campaign.

VII. Conclusion

The Mars Helicopter is an ambitious, first-of-its-kind technology demonstration mission concept that would collect aerial reconnaissance data during repeated short duration flights on Mars. For the design to be feasible, the helicopter must be lightweight and conserve energy. These requirements result in a delicate balance for the thermal design: the helicopter must absorb as much heat in the daytime without overheating the batteries while limiting heater energy needed to survive in the nightttime. These requirements are met primarily by thermally decoupling the batteries and electronics, which have the driving AFT limits in the helicopter, from the larger temperature variations experienced by the fuselage and external components. Using a fuselage coating with high α/ε helps to absorb daytime heating while minimizing radiation heat loss at night. Thermal balance testing of an engineering model enabled correlation of the analytical thermal model. Model predictions for an improved post-test thermal design demonstrate that energy and temperature requirements can be met with margin at the northern landing site under consideration. The Mars Helicopter will continue with design improvements, fabrication, and testing and then wait for a suitable mission to hitchhike to Mars.

Acknowledgments

The research was carried out at the Jet Propulsion Laboratory, California Institute of Technology, under a contract with the National Aeronatutics and Space Administration. The author would like to acknowledge the efforts of all the thermal engineers who have worked on this thermal design and provided inputs to the manuscript. Government Sponsorship Acknowledged.

References

[1]Kliore, A., Cain, D. L., Levy, G. S., Eshleman, V. R., Fjelbo, G., Drake, F. D., "Occultation Experiment: Results of the First Direct Measurement of Mars's Atmosphere and Ionosphere," Science, Vol 149, No 3689, 10 Sept. 1965, pp 1243-1248.

[2]Novak, K., Phillips, C., Sunada, E., Kinsella, G., "Mars Exploration Rover Surface Mission Flight Thermal Performance," *35th International Conference on Environmental Systems*, Rome, Italy, July 11-14, 2005.

[3]Golombek, M., Kipp, D., Warner, N., Daubar, I., Fergason, R., Kirk, R., Beyer, R., Huertas, A., Piqueux, S., Putzig, N., Campbell, B., Morgan, G., Charalambous, C., Pike, W., Gwinner, K., Calef, F., Kass, D., Mischna, M., Ashley, J., Bloom, C., Wigton, N., Hare, T., Schwartz, C., Gengl, H., Redmond, L., Trautman, M., Sweeney, J., Grima, C., Smith, I., Sklyanskiy, E., Lisano, M., Benardini, J., Smrekar, S., Lognonné, P., Banerdt, W., "Selection of the InSight Landing Site," Space Science Review, Vol. 211, 14 Dec. 2016, pp 5-95.

[4]Golombek, M., Grant, J., Kipp, D., Vasavada, A., Kirk, R., Fergason R., Bellutta, P., Calef, F., Larsen, K., Katayama Y., Huertas, A., Beyer, R., Chen, A., Parker, T., Pollard, B., Lee, S., Sun, Y., Hoover, R., Sladek, H., Grotzinger J., Welch R., Noe Dobrea E., Michalski, J., Watkins, M., "Selection of the Mars Science Laboratory Landing Site," Space Science Review, Vol. 170, 21 July, 2012, pp 641-737.

[5]Redmond, M., Sherman, S., Bhandari, P., Novak, K., "Thermal Design, Analysis, and Sensitivity of a Sample Tube on the Martian Surface," *47th International Conference on Environmental Systems*, Charleston, SC, July 16-20, 2017.

[6]Bhandari, P., Karlmann, P., Anderson, K., Novak, K., "CO2 Insulation for Thermal Control of the Mars Science Laboratory," *41st International Conference on Environmental Systems*, Portland, OR, July 17-21, 2011.

[7]Novak, K. S., Phillips, C. J., Birur, G. C., Sunada, E. T., Pauken, M. T., "Development of a Thermal Control Architecture for the Mars Exploration Rovers," *Space Technology Applications International Forum*, Institute for Space and Nuclear Power Studies, Vol. 1, Albuquerque, NM, 2003.